

Stationary components of He I in strong magnetic fields – a tool to identify magnetic DB white dwarfs

S. Jordan¹, P. Schmelcher², and W. Becken²

¹ Institut für Theoretische Physik und Astrophysik, D-24098 Kiel, Germany
e-mail: jordan@astrophysik.uni-kiel.de

² Institut für Physikalische Chemie, Im Neuenheimer Feld 229, D-69120 Heidelberg, Germany
e-mail: peter@tc.pci.uni-heidelberg.de

Abstract. In only three of the 61 known magnetic white dwarfs helium has been identified unambiguously while about 20% of all non-magnetic stars of this class are known to contain He I or He II. One reason for this discrepancy is that the identification of peculiar objects as magnetic white dwarfs is based either on the presence of hydrogen line components in strong magnetic fields — for which atomic data exist since 1984 — or the polarization of the corresponding radiation which has not been measured for many objects. Until recently, data for He I data were available only for magnetic fields below 20 MG. This changed with the publication of extensive data by the group in Heidelberg. The corresponding calculations have now been completed for the energetically lowest five states of singlet and triplet symmetry for the subspaces with $|m| \leq 3$; selected calculations have been performed for even higher excitations. In strongly magnetized white dwarfs only line components are visible whose wavelengths vary slowly with respect to the magnetic field, particularly stationary components which have a wavelength minimum or maximum in the range of the magnetic fields strengths on the stellar surface. In view of the many ongoing surveys finding white dwarfs we want to provide the astronomical community with a tool to identify helium in white dwarfs for fields up to 5.3 GG. To this end we present all calculated helium line components whose wavelengths in the UV, optical, and near IR vary slowly enough with respect to the field strength to produce visible absorption features. We also list all stationary line components in this spectral range. Finally, we find series of minima and maxima which occur as a result of series of extremal transitions to increasingly higher excitations. We estimated the limits for 8 series which can possibly give rise to additional absorption in white dwarf spectra; one strong absorption feature in GD229 which is yet unexplained by stationary components is very close to two estimated series limits.

Key words. stars: white dwarfs – stars: magnetic fields – stars: individual: GD 229

1. Introduction

In about 3-4% of all white dwarfs magnetic fields have been detected ranging from 2 kG in 40 Eri B (Fabrika & Valyavin 1999) up to 1 GG (Schmidt et al. 1986, Latter et al. 1987) in the case of PG 1031+234. 15 of these 61 objects (Wickramasinghe & Ferrario 2000, Jordan 2001) have fields in excess of 100 MG making them comparable to the typical field strengths found in millisecond pulsars. Since their magnetic fields considerably exceed what can be produced in terrestrial laboratories they represent cosmic laboratories that probe the behaviour and properties of atoms and molecules under such extreme conditions (for reviews of the subject see Ruder et al 1994 and Schmelcher & Schweizer 1998).

Until 1984 atomic data for hydrogen were limited to field strengths below 20 MG (Kemic 1974) and above

10^{10} G (Garstang 1977) and it was a pure speculation that the unidentified shallow “Minkowski bands” (Minkowski 1938) in the spectrum of Grw +70°8247 were due to magnetic fields. The detection of circular polarization (Kemp 1970) showed that a magnetic field exists on this star. The strength, however, could not be determined until Forster et al. (1984) and Henry & O’Connell (1984) published energy level shifts and transition probabilities for line components of hydrogen in the intermediate-field range.

Particularly, the so called stationary line components, which go through maxima or minima as functions of the magnetic field strength lead to significant absorption structures. Lines whose behavior is monotonic and whose wavelengths change significantly with the field strength are smeared out due to the inhomogeneous magnetic field over the surface of the white dwarfs. The identification of the stationary components of hydrogen led to an estimation of the approximate range of field strengths cover-

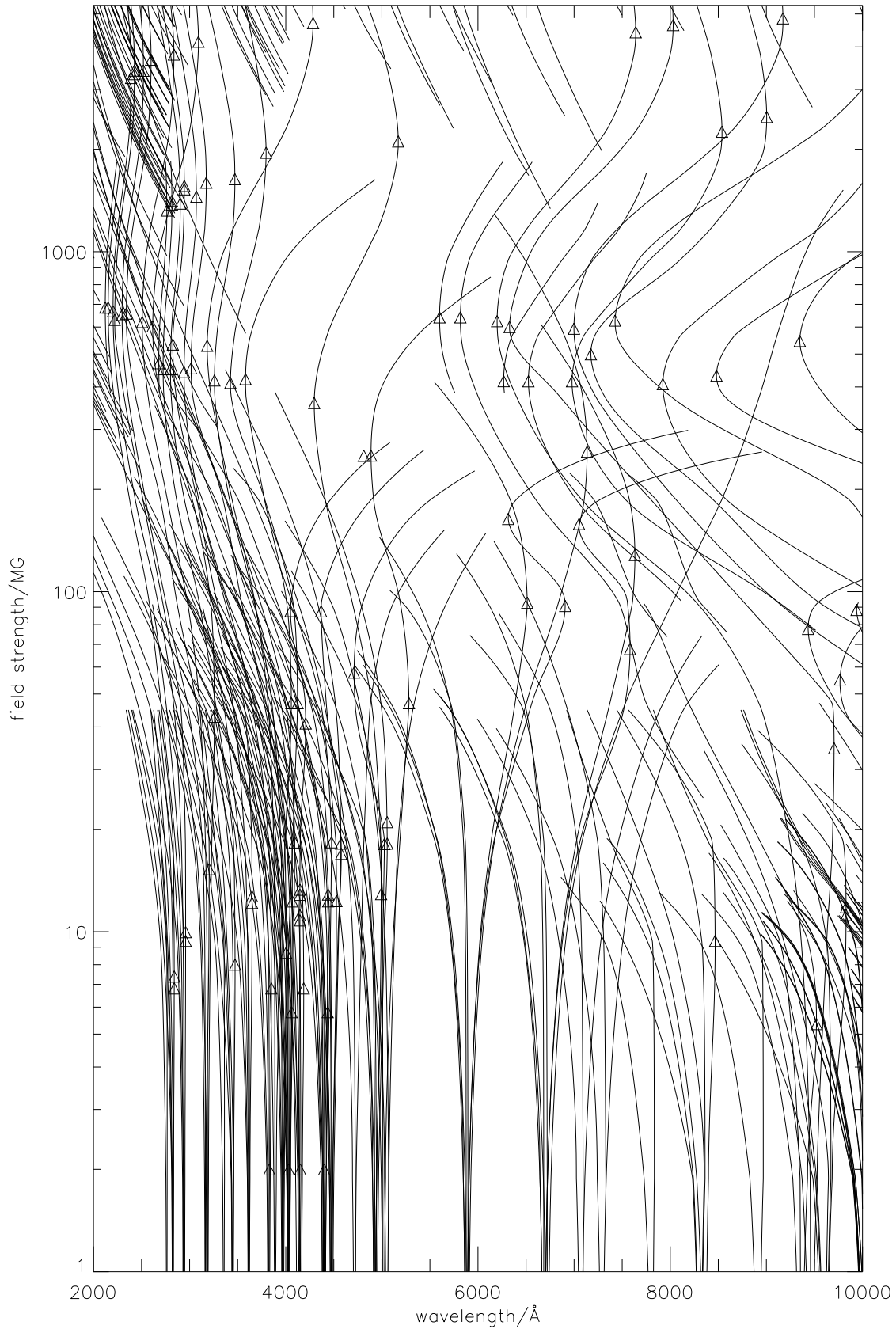


Fig. 1. Wavelengths of all calculated stationary line components of He I (minimum or maximum wavelengths are marked by triangles) and, additionally, of all other components which vary by less than 500 \AA while the magnetic field changes by more than a factor of two. Note the extremely large number of stationary components between 300 and 700 MG corresponding to the field strength of GD 229

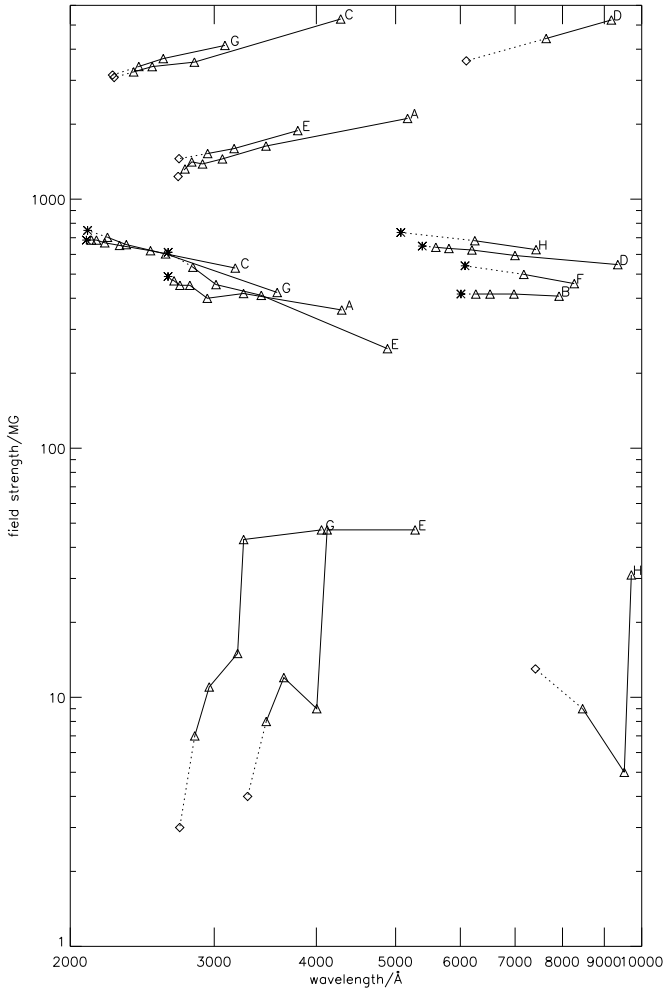


Fig. 2. Positions of the stationary components of the series A–H (triangles) and the estimated series limits (asterisk for limits of minima, squares for limits of maxima)

ing the stellar surface of Grw +70°8247: 150 to 500 MG (Greenstein 1984, Greenstein et al. 1985, Angel et al. 1985, Wunner et al. 1985) and identified the star as spectral type DAP. Later, Grw +70°8247 and other magnetic white dwarfs have been analyzed with more sophisticated methods using detailed simulations for the radiative transfer through magnetized stellar atmospheres (Wickramasinghe & Ferrario 1988; 1989). However, the basic explanation and the approximate field strengths could be inferred from a simple comparison of the position of absorption features with the lists of stationary line components for hydrogen.

Until recently, no reliable atomic data for the intermediate range of magnetic field strengths existed for neutral helium. Only in the case of Feige 7 Achilleos et al. (1992) could identify He I besides hydrogen in an off-centered dipole field of strength 35 MG with an extrapolation of the Kemic (1974) data. On the other hand several objects – suspected to be magnetic due to the strange spectral features and their polarization — remained unexplained.

Even for the simplest atom i.e. hydrogen an investigation of its electronic structure is very intricate in the presence of a strong magnetic field. The degrees of freedom perpendicular and parallel to the external field cannot be separated but mix strongly. The latter is due to the competition of the Coulomb and magnetic interaction which possess different symmetries. Energetically low-lying levels can easily be obtained only for fields $0.01 > \gamma = B/2.35 \cdot 10^9$ G (Zeeman and Paschen-Back regime) where perturbation theory applies or for $\gamma \gg 1$ where the dominant magnetic interaction perpendicular to the field leads to an approximate adiabatic separation of the variables. In the case of helium the situation is significantly more complicated due to the electron-electron interaction. First calculations of helium atoms in the intermediate field regime (Braun et al. 1998, Jones et al. 1997, Ruder et al. 1994 and references therein) either lacked the accuracy or could access only a few excited states of certain selected symmetries and for a few selected field strengths. As a consequence a direct comparison with observed spectra from magnetic white dwarfs was not possible. This changed not before Becken et al. (1999) and Becken & Schmelcher (2000) published a large grid of atomic data for helium at arbitrary magnetic field strengths.

The most famous example of a suspected helium rich magnetic white dwarf was GD 229 having a large number of strong absorption features in the optical and UV. With the help of the newly available data Jordan et al. (1998) could attribute most of the absorption structures in the spectrum with stationary components of neutral helium in a range of magnetic fields between 300 and 700 MG.

The number of magnetic white dwarfs with clearly identified helium lines is still very small: Besides Feige 7 and GD 229 He I could only be identified (Jordan 2001) in HE0241-0155 ($B \lesssim 25$ MG) and with less certainty in HE 1211-1707 ($20 < B < 150$ MG).

Without reliable atomic data Reimers et al. (1998) have tentatively identified He I at a field strength between 20 and 30 MG in HE 0107-0158, HE 0026–2150, and HE 0003–5701. However, it now turned out that this conclusion could be discarded after applying our more accurate atomic data; probably these systems are binary stars of which one component is a subdwarf.

Since the publications by Becken et al. (1999) and Becken & Schmelcher (2000) the data for helium in strong magnetic fields have now been completed for all transitions between the five lowest energy levels with magnetic quantum numbers $m = -3, -2, -1, 0, +1, +2, +3$ for both spin singlet and triplet states and for both z-parities with the exclusion of the negative z-parity states for $m = 3$. To obtain certain desired stationaryities even higher i.e. the sixth and seventh excitations of certain symmetries have been investigated (see below). Apart from this we have slightly improved the accuracy of our previous results by enlarging the corresponding basis sets employed in the electronic structure calculations.

The whole data set for He I comprises of about 2000 line components. With this paper we want to provide the astronomical community with an up-to-date overview of all calculated stationary and slowly varying line components of helium in the regimes of field strengths relevant for magnetic white dwarfs. This is particularly useful for an identification of helium-rich magnetic white dwarfs expected to be found by the large number of ongoing surveys (e.g. Sloan Digital Sky Survey, York et al. 2001; Hamburg ESO Survey, Wisotzki et al. 1996; Hamburg Quasar Survey, Hagen et al. 1995; Edinburgh Cape Survey, Stobie et al. 1997; Montreal Cambridge Tololo Survey, Lamontagne et al. 2000; Second Byurakan Survey, Stepanian 1999).

2. Helium atom in strong magnetic fields

The electronic Hamiltonian of the helium atom for fixed nucleus and subjected to a strong magnetic field is given by

$$\mathcal{H} = \sum_{i=1}^2 \left(\frac{1}{2m} \mathbf{p}_i^2 - \frac{e}{2m} B L_{z_i} + \frac{e^2}{8m} B^2 (x_i^2 + y_i^2) - \frac{2e^2}{|\mathbf{r}_i|} - \frac{e}{m} B S_{z_i} \right) + \frac{e^2}{|\mathbf{r}_1 - \mathbf{r}_2|}. \quad (1)$$

The magnetic field is oriented along the z -axis. The respective terms describe the field-free kinetic energy, the orbital Zeeman term, the diamagnetic interaction, the Coulomb attraction, the spin Zeeman energies, and the repulsive electron-electron interaction. Results beyond the presently applied fixed nucleus approximation can be obtained via the corresponding scaling relations (Becken & Schmelcher 2000).

The main advantage of our calculations is the use of an extremely flexible basis set of anisotropic orbitals with nonlinear variational parameters $\{\alpha_i, \beta_i\}$ which are adjusted i.e. optimized for each magnetic field strength:

$$\Phi_i(\rho, \phi, z) = \rho^{n_{\rho_i}} z^{n_{z_i}} \exp(-\alpha_i \rho^2 - \beta_i z^2) \exp(im_i \phi) \quad (2)$$

where $n_{\rho_i} = |m_i| + 2k_i$, $n_{z_i} = \pi_{z_i} + 2l_i$ with $k_i, l_i = 0, 1, 2, \dots$. $\{\alpha_i, \beta_i\}$ are nonlinear variational parameters; π_{z_i} is the z parity of the one particle function. For the investigation of the electronic structure of the helium atom we built from the above optimized atomic orbitals the corresponding symmetry adapted two-particle configurations and represent the Hamiltonian matrix in these configurations (the typical dimension of the full matrices is 5000). To this end a fast and accurate evaluation of the corresponding electron-electron matrix elements is crucial. A number of advanced analytical as well as numerical techniques have been employed to achieve this goal. For details on the latter we refer the reader to Becken et al. (1999) and Becken & Schmelcher (2000). To obtain the eigenenergies and eigenfunctions of the atom a full configuration interaction approach is used. Due to the nonorthogonality of the above basis set the latter leads to a generalized eigenvalue problem which can be diagonalized using standard library routines. We remark that it is only due to

the above-indicated extensive developmental work that a series production of accurate atomic data for the helium atom in the presence of the strong field became possible.

In the presence of a magnetic field the total angular momentum of the atom is not conserved and provides therefore not a good quantum number. The only remaining spatial constant of motion is the projection of the total angular momentum $\sum_i L_{z_i}$ onto the magnetic field axis (quantum number M). Furthermore the total z -parity ($\Pi_z : z_i \rightarrow -z_i$) represents a symmetry of the atom (total parity is also conserved but can be obtained from the previous symmetries). The spin symmetries ($S = 1, 3$ for singlet and triplet, respectively) are the same as in the absence of a magnetic field. We therefore use the spectroscopic notation $n^S M^{\Pi_z}$ where n indicates the energetical degree of excitation.

3. Stationary components

Stationary components remain visible i.e. may lead to absorption edges in the observed spectra even when the magnetic field strength varies considerably over the surface of a white dwarf.

Table 1 lists all 101 singlet and triplet stationary line components of He I with $|m| \leq 3$ and for both z -parities (for $|m| = 3$ only the positive z parity has been considered). Included are those transitions whose wavelengths belong to the regime from the FUV ($> 900 \text{ \AA}$) to the near infrared ($< 10000 \text{ \AA}$) and run through minima or maxima with respect to the varying magnetic field strength. No stationary components were found in the regime 900-2100 \AA . The white dwarf with the highest field strength discovered so far, PG 1031+234, has a maximum field strength of about 1 GG; to be on the safe side concerning possible higher field strengths we have listed in Table 1 all stationary components up to 5.3 GG.

Stationarity is not a necessary condition for line components to produce visible absorption features; therefore we also looked for components whose wavelengths are not stationary but do not change by more than 500 \AA for a variation of the magnetic field by more than a factor of two (corresponding to the spread of centered dipole fields from the magnetic pole to the equator). We expect the latter to be also candidates for observable absorption edges. In Fig. 1 the wavelengths of these components are shown together with the stationary ones for varying magnetic field strength. The uncertainties of the calculated wavelengths are smaller than a few \AA . However, since the lines are interpolated on a grid for 20 different magnetic field strengths the typical accuracy with respect to the position of the minima or maxima is about 10 \AA ; only in a few cases the error can go up to 50 \AA . These values were estimated by comparing the results of different interpolation schemes. In the case of GD 229 26 stationary components could be identified in the optical and UV spectrum in Jordan et al. 1998. Such a rich spectrum is probably an exception since the number of stationary line components in the range of magnetic fields between 300

and 700 MG is much larger than in any other comparable range of magnetic field strengths. On the other hand we expect a priori that in the intermediate regime of field strengths a severe rearrangement of the electronic wave functions takes place and therefore a strong dependence of the energy levels on the field strength has also to be expected (the above mentioned interval 300 to 700 MG is contained in the intermediate regime). Since the publication by Jordan et al. (1998), which analyzed line components for $|m| \leq 1$, the investigations on the electronic eigenstates of the helium atom in a magnetic field proceeded significantly and in particular a large number of higher excited states covering new symmetries have been studied (see above). As a consequence seven new extrema have been obtained in the interval 300 to 700 MG. They possess the wavelengths 2204, 2679, 2724, 5600, 5810, 6267 Å and 6524 Å. With the exception of the wavelength 5810 Å these new extrema also match nicely with the absorption features of the magnetic white dwarf GD 229 which confirms our previous conclusion of strong evidence for helium on this white dwarf.

However, not everything is completely clarified concerning the spectrum of GD 229 even within the framework of its interpretation in terms of stationary transitions. The strong absorption feature at 4000 – 4200 Å is met 'only' by the stationary transition $2^1 0^+ \rightarrow 2^1 0^-$ which cannot account for absorption at $\lambda < 4296$ Å. Furthermore the absorption edge at approximately 5280 Å has no stationary counterpart even within the significantly enlarged data set of atomic calculations. A careful look at the stationary atomic line components particularly relevant for the interpretation of GD 229 (300 to 700 MG), however, reveals that these stationarities occur in terms of series of transitions to increasingly higher excitations. The series (see Table 1) are

$$\begin{aligned}
 A: & 2^1 0^+ \rightarrow n^1 0^-, n \geq 2 \\
 B: & 3^1 0^+ \rightarrow n^1 0^-, n \geq 3 \\
 C: & 1^3 0^+ \rightarrow n^3 0^-, n \geq 2 \\
 D: & 2^3 0^+ \rightarrow n^3 0^-, n \geq 3 \\
 E: & 2^1 0^+ \rightarrow n^1 (-1)^+, n \geq 2 \\
 F: & 3^1 0^+ \rightarrow n^1 (-1)^+, n \geq 4 \\
 G: & 1^3 0^+ \rightarrow n^3 (-1)^+, n \geq 2 \\
 H: & 2^3 0^+ \rightarrow n^3 (-1)^+, n \geq 4
 \end{aligned} \tag{3}$$

Although an ab initio electronic structure investigation can always reliably calculate only a finite number of excitations it suggests itself that the complete above series for arbitrary n lead to stationarities. Within our atomic calculations we could show the stationary character of the corresponding transitions for $n \leq 7$ for the states of the $1^0-, 3^0-$ subspaces and for $n \leq 5$ for the subspaces $1^1(-1)^+, 3^1(-1)^+$. Let us explain the above statement in more detail for the series D i.e.

$2^3 0^+ \rightarrow n^3 0^-$. The corresponding stationary wavelengths are 9348, 6998, 6199, 5810, 5600 Å for $n = 3 - 7$. This shows exemplary that the series of stationarities converges towards a series limit at which there is an infinite accumulation of stationarities. This property seems to hold for all of the above series and is an amazing fact of the electronic structure of the atom in the considered particular part of the intermediate regime of field strengths. The presence of the infinite series of stationarities can be further elucidated by observing that the energies of the initial states $2^1 0^+, 3^1 0^+, 1^3 0^+, 2^3 0^+, 2^1 0^+, 3^1 0^+, 1^3 0^+, 2^3 0^+$ of the series A–H show already the corresponding minima and maxima responsible for the series of stationarities. Due to the dominating dependence of the energies of these low-lying states on the field strength they leave their fingerprint on any transition to higher excited states which as a consequence become stationary for a certain field strength. From the available atomic data we can now estimate the wavelengths of the series limits by using the empirical law that the wavelengths become smaller by a factor of two for successive transitions for high n . For the series A–H the limiting wavelengths are listed in Table 2. Fig. 2 shows that this rule applies well for all stationary components above 100 MG. We remark that the series limits of F and H are particularly crude estimates. Nevertheless these estimates nicely fit with the position of major absorption edges in the spectrum of GD 229 and in particular the estimated series limits of D and H (5390 and 5074 Å, respectively) come very close to the so far unexplained absorption edge at approximately 5300 Å. In view of the above one can conjecture that the accumulation of stationarities might be responsible for certain observed features of the spectrum. Future calculations on the oscillator strengths of the stationary line components will certainly help to further clarify this problem. The role of bound-free transitions for the helium atom in the presence of the strong field and in particular its impact on observable spectra from white dwarf atmospheres is equally an open question. The corresponding investigations require however major theoretical and computational developments. Generally it is assumed that the higher excited states are strongly de-populated by the interaction of close atoms in the high density atmospheres of the white dwarfs.

Of course we cannot strictly exclude that further relevant stationary line components arise due to the transitions involving other symmetry subspaces and states than those discussed above. However according to the previous discussion the regularity with respect to the emergence of stationary transitions particularly in the field regime 300 to 700 MG suggests that all major components have been addressed. Additionally one has to keep in mind that the level spacing decreases rapidly with increasing magnetic quantum numbers for the states involved and therefore the wavelength of the corresponding transitions become increasingly larger and are not of relevance to the observed spectral range. For example, the series of circular polarized transitions $1^1(-2)^+ \rightarrow n^1(-3)^+, n = 1 - 5$ possesses stationarities for the wavelengths 21400, 13000, 11000, 10900

and 10000Å, respectively, which excludes it from the spectral regime considered here. Even higher excitations $n \geq 6$ will not be significantly below 10000Å. These arguments hold for both singlet and triplet excitations: with increasing degree of excitation the singlet and triplet splitting decreases rapidly. A similar argument holds also for the linear polarized stationary transitions like e.g. $3^1(-2)^+ \rightarrow n^1(-2)^-, n \geq 2$. This tendency is even enforced for the corresponding transitions involving the $|m| \geq 4$ subspaces. We emphasize that the above arguments are valid in the regime of field strengths considered here i.e. for $B \leq 5.3$ GG. In the high-field regime $B \geq 10$ GG severe changes can be observed.

Some remarks are in order concerning a recent work which suggests an alternative interpretation of the spectrum of GD 229. Jones et al (1999) used their results on helium calculations in strong fields in order to conclude that both He I as well as He II could contribute to the observed spectrum. However the authors dealt with a significantly smaller set of atomic data and therefore missed many of the stationarities given in the present work. Moreover their explanation is based on the existence of He II in the atmosphere of GD 229 which is a critical issue since the effective temperature (about 16000 K according to Schmidt et al. 1990) is generally not assumed to be large enough in order to expect He II; in non-magnetic white dwarfs models predict He II to occur at T_{rmeff} above about 28000 K. To allow, nevertheless, for the existence of He II a double excitation process via a single UV photon followed by a subsequent radiationless autoionizing process is suggested. To the authors of the present work the efficiency of this mechanism is very questionable.

4. Outlook

With the data presented in this work it will be possible for observational astronomers to perform a first identification and get evidence for helium in magnetic white dwarfs. This is particularly important due to the large number of magnetic objects being discovered by many (ongoing) surveys to find stellar and extragalactic objects. A positive identification must be based on the simultaneous assignment of slowly varying or stationary line components in a realistic range of magnetic field strengths. Although this on its own does not allow a prediction of the strengths of the absorption features it provides a good starting point for the parameters relevant to subsequent numerical calculations of the polarized radiation of magnetic white dwarfs. The latter can be directly compared to the spectra and polarization measurements. We are currently working on the inclusion of the energies, wavelengths, and transition probabilities for all calculated line components for neutral helium in arbitrary magnetic fields into our models for the radiative transfer.

From our comprehensive data set it became clear that GD 229 with its large number of absorption features is a very special object since the regime of field strengths covering its surface (≈ 300 -700 MG) contains a stronger

accumulation of stationary transitions of He I than any other equally large interval of field strengths.

Acknowledgements. The Deutsche Studienstiftung and the Deutsche Forschungsgemeinschaft (Schm 885/7-1 & Ko 738/7-1) are gratefully acknowledged for financial support.

References

- Achilleos, N., Wickramasinghe, D.T., Liebert, J., Saffer, R.A., Grauer, A.D. 1992, ApJ 396, 273
 Angel, J.R.P. Liebert, J., Stockman, H.S. 1985, ApJ 292, 260
 Becken, W., Schmelcher, P., Diakonou, F.K. 1999, J.Phys. B 32, 1557
 Becken, W., Schmelcher, P. 2000, J.Phys. B 33, 545; acc.f.publ. in Phys.Rev.A 2001
 Braun M., Schweizer W., Elster H., 1998, Phys.Rev.A 57, 3739
 Fabrika, S., Valyavin, G. 1999, ASP Conf. Ser. 169, eds. Solheim & Meistas, p. 225
 Forster, H., Strupat, W., Rösner, W., Wunner, G., Ruder, H., Herold, H., 1984, J.Phys., V 17, 1301
 Garstang, R.H. 1977, Rep.Prog.Phys. 40, 105
 Greenstein, J.L. 1984, ApJL 281, L47
 Greenstein, J.L., Henry, R.J.W., O'Connell, R.F. 1985, ApJL 289, L25
 Hagen H.-J., Groote D., Engels D. & Reimers D. 1995, A&AS 111, 195
 Jones M.D., Ortiz G., Ceperley D.M., 1997, Phys.Rev.E 55, 6202; Phys.Rev.A 59, 2875 (1999)
 Jones M.D., Ortiz G., Ceperley D.M., 1999, A&A 343, L91
 Jordan, S. 1989, in White Dwarfs, Lecture Notes in Physics 328, ed. G. Wegner, Springer-Verlag, New York, p. 333
 Jordan, S., Schmelcher, P., Becken, W., Schweizer, W. 1998, A&A 336, L33
 Jordan, S. 2001, ASP Conference Series, Vol. XXX, H.L. Shipman & J.L. Provencal, eds., in press
 Henry, R.J.W., O'Connell, R.F. 1984, ApJ 282, L97
 Kemic, S.B. 1974, JILA Rep. 133
 Kemp, J.C. 1970, ApJ 162, 169
 Latter, W. B., Schmidt, G.D., Green, R.F. 1987, ApJ 320, 308
 Lamontagne R., Demers S., Wesemael F., Fontaine G. & Irwin M. J. 2000, AJ 119, 241
 Minkowski, R. 1938, Annu.Rep.Mt.Wilson Obs., p.38
 Reimers, D., Jordan, S., Beckmann, V., Christlieb, N., Wisotzki, L., 1998, A&A 337, L13
 Wisotzki L., Köhler T., Groote D. & Reimers D. 1996, A&A 115, 227
 Ruder H., Wunner G., Herold H., Geyer F., 1994 Atoms in Strong Magnetic Fields, Springer Verlag
 P. Schmelcher and W. Schweizer (Eds.), Atoms and Molecules in Strong External Fields, Plenum Press 1998
 Schmidt, G.D., West, S.C., Liebert, J., Green, R.F., Stockman, H.S. 1986, ApJ 309, 218
 Schmidt, G.D., Latter, W.B., Foltz, C.B., 1990, ApJ 350, 758
 Stepanian J.A., Chavushyan V.H., Carrasco L., Tovmassian H.M. & Erastova L.K. 1999, PASP, 111, 1099
 Stobie R.S., Kilkenny D., O'Donoghue D. et al. 1997, MNRAS 287, 848
 Wickramasinghe, D.T., Ferrario, L. 1988, ApJ, 327, 222
 Wickramasinghe, D.T., Ferrario, L., 2000 PASP 112, 873
 Wunner, G., Rösner, W., Herold, H., Ruder, H. 1985, A&A 149, 102
 York, D.G., et al. 2000, AJ 120, 1579

Table 1. Line components of He I which are stationary at wavelengths between 900 and 10000 Å for magnetic fields below 5.3 GG sorted by the wavelength of the minimum or maximum, respectively. Note that the wavelengths (and corresponding field strengths) of the minima and maxima are interpolated in a relatively crude grid for 20 different field strengths so that the accuracy of the wavelengths varies between about 10 and 50 Å. The membership to the series A–H (see Eq. 3) is also indicated.

	B/MG	$\lambda/\text{Å}$	zero field trans.	transition	type
C:	685	2123	$2^3S_0 \rightarrow 6^3P_0$	$1^30^+ \rightarrow 7^30^-$	min
C:	685	2153	$2^3S_0 \rightarrow 5^3F_0$	$1^30^+ \rightarrow 6^30^-$	min
C:	668	2204	$2^3S_0 \rightarrow 5^3P_0$	$1^30^+ \rightarrow 5^30^-$	min
G:	703	2221	$2^3S_0 \rightarrow 5^3P_{-1}$	$1^30^+ \rightarrow 5^3(-1)^+$	min
C:	652	2298	$2^3S_0 \rightarrow 4^3F_0$	$1^30^+ \rightarrow 4^30^-$	min
G:	657	2342	$2^3S_0 \rightarrow 4^3F_{-1}$	$1^30^+ \rightarrow 4^3(-1)^+$	min
C:	3243	2391	$2^3S_0 \rightarrow 5^3P_0$	$1^30^+ \rightarrow 5^30^-$	max
G:	3409	2426	$2^3S_0 \rightarrow 5^3P_{-1}$	$1^30^+ \rightarrow 5^3(-1)^+$	max
C:	621	2507	$2^3S_0 \rightarrow 4^3P_0$	$1^30^+ \rightarrow 3^30^-$	min
C:	3406	2519	$2^3S_0 \rightarrow 4^3F_0$	$1^30^+ \rightarrow 4^30^-$	max
G:	3668	2599	$2^3S_0 \rightarrow 4^3F_{-1}$	$1^30^+ \rightarrow 4^3(-1)^+$	max
A:	603	2616	$2^3S_0 \rightarrow 4^3P_{-1}$	$1^30^+ \rightarrow 3^3(-1)^+$	min
A:	470	2679	$2^1S_0 \rightarrow 6^1F_0$	$2^10^+ \rightarrow 7^10^-$	min
A:	451	2724	$2^1S_0 \rightarrow 5^1P_0$	$2^10^+ \rightarrow 6^10^-$	min
A:	1322	2763	$2^1S_0 \rightarrow 6^1F_0$	$2^10^+ \rightarrow 7^10^-$	max
A:	451	2801	$2^1S_0 \rightarrow 5^1F_0$	$2^10^+ \rightarrow 5^10^-$	min
A:	1411	2816	$2^1S_0 \rightarrow 5^1P_0$	$2^10^+ \rightarrow 6^10^-$	max
E:	533	2825	$2^1S_0 \rightarrow 5^1F_{-1}$	$2^10^+ \rightarrow 5^1(-1)^+$	min
C:	3549	2837	$2^3S_0 \rightarrow 4^3P_0$	$1^30^+ \rightarrow 3^30^-$	max
G:	7	2840	$2^3S_0 \rightarrow 6^3P_{-1}$	$1^30^+ \rightarrow 7^3(-1)^+$	max
A:	1385	2903	$2^1S_0 \rightarrow 5^1F_0$	$2^10^+ \rightarrow 5^10^-$	max
A:	400	2942	$2^1S_0 \rightarrow 4^1P_0$	$2^10^+ \rightarrow 4^10^-$	min
E:	1525	2945	$2^1S_0 \rightarrow 5^1F_{-1}$	$2^10^+ \rightarrow 5^1(-1)^+$	max
G:	11	2958	$2^3S_0 \rightarrow 5^3P_{-1}$	$1^30^+ \rightarrow 5^3(-1)^+$	max
E:	454	3015	$2^1S_0 \rightarrow 4^1P_{-1}$	$2^10^+ \rightarrow 4^1(-1)^+$	min
A:	1451	3070	$2^1S_0 \rightarrow 4^1P_0$	$2^10^+ \rightarrow 4^10^-$	max
G:	4142	3092	$2^3S_0 \rightarrow 4^3P_{-1}$	$1^30^+ \rightarrow 3^3(-1)^+$	max
E:	1596	3173	$2^1S_0 \rightarrow 4^1P_{-1}$	$2^10^+ \rightarrow 4^1(-1)^+$	max
C:	529	3183	$2^3S_0 \rightarrow 3^3P_0$	$1^30^+ \rightarrow 2^30^-$	min
G:	15	3204	$2^3S_0 \rightarrow 4^3F_{-1}$	$1^30^+ \rightarrow 4^3(-1)^+$	max
A:	418	3258	$2^1S_0 \rightarrow 4^1F_0$	$2^10^+ \rightarrow 3^10^-$	min
G:	43	3259	$2^3S_0 \rightarrow 4^3P_{-1}$	$1^30^+ \rightarrow 3^3(-1)^+$	max
E:	411	3425	$2^1S_0 \rightarrow 4^1F_{-1}$	$2^10^+ \rightarrow 3^1(-1)^+$	min
A:	1634	3471	$2^1S_0 \rightarrow 4^1F_0$	$2^10^+ \rightarrow 3^10^-$	max
E:	8	3473	$2^1S_0 \rightarrow 6^1F_{-1}$	$2^10^+ \rightarrow 7^1(-1)^+$	max
G:	422	3582	$2^3S_0 \rightarrow 3^3P_{-1}$	$1^30^+ \rightarrow 2^3(-1)^+$	min
E:	12	3650	$2^1S_0 \rightarrow 5^1F_{-1}$	$2^10^+ \rightarrow 5^1(-1)^+$	max
E:	1885	3796	$2^1S_0 \rightarrow 4^1F_{-1}$	$2^10^+ \rightarrow 3^1(-1)^+$	max
	2	3830	$2^3P_{-1} \rightarrow 6^3D_{-2}$	$1^3(-1)^+ \rightarrow 5^3(-2)^+$	max
	7	3851	$2^3P_0 \rightarrow 6^3D_{-1}$	$1^30^- \rightarrow 5^3(-1)^-$	max
E:	9	4004	$2^1S_0 \rightarrow 4^1P_{-1}$	$2^10^+ \rightarrow 4^1(-1)^+$	max
	2	4030	$2^3P_{-1} \rightarrow 6^3D_{-2}$	$1^3(-1)^+ \rightarrow 4^3(-2)^+$	max
	88	4050	$5^3S_0 \rightarrow 2^3P_{+1}$	$6^30^+ \rightarrow 1^3(+1)^+$	min
G:	47	4058	$2^3S_0 \rightarrow 3^3P_{-1}$	$1^30^+ \rightarrow 2^3(-1)^+$	max
	6	4061	$2^3P_0 \rightarrow 5^3G_{-1}$	$1^30^- \rightarrow 4^3(-1)^-$	max
	12	4060	$2^3P_{-1} \rightarrow 5^3D_{-2}$	$1^3(-1)^+ \rightarrow 3^3(-2)^+$	max
	18	4094	$2^3P_0 \rightarrow 5^3D_{-1}$	$1^30^- \rightarrow 3^3(-1)^-$	max
E:	47	4123	$2^1S_0 \rightarrow 4^1F_{-1}$	$2^10^+ \rightarrow 3^1(-1)^+$	max
	13	4147	$5^3S_0 \rightarrow 2^3P_{+1}$	$6^30^+ \rightarrow 1^3(+1)^+$	min
	2	4150	$2^1P_{-1} \rightarrow 6^1D_{-2}$	$1^1(-1)^+ \rightarrow 5^1(-2)^+$	max
	7	4187	$2^1P_0 \rightarrow 6^1D_{-1}$	$1^10^- \rightarrow 5^1(-1)^-$	max
	41	4208	$5^3S_0 \rightarrow 2^3P_{+1}$	$6^30^+ \rightarrow 1^3(+1)^+$	max
C:	5288	4284	$2^3S_0 \rightarrow 3^3P_0$	$1^30^+ \rightarrow 2^30^-$	max
	359	4296	$2^1S_0 \rightarrow 3^1P_0$	$2^10^+ \rightarrow 2^10^-$	min
A:	88	4368	$4^3D_0 \rightarrow 2^3P_{+1}$	$5^30^+ \rightarrow 1^3(+1)^+$	min
	2	4400	$2^1P_{-1} \rightarrow 5^1G_{-2}$	$1^1(-1)^+ \rightarrow 4^1(-2)^+$	max
	5	4442	$2^1P_0 \rightarrow 5^1G_{-1}$	$1^10^- \rightarrow 4^1(-1)^-$	max
	13	4441	$2^1P_{-1} \rightarrow 5^1D_{-2}$	$1^1(-1)^+ \rightarrow 3^1(-2)^+$	max
	18	4477	$2^1P_0 \rightarrow 5^1D_{-1}$	$1^10^- \rightarrow 3^1(-1)^-$	max
	12	4528	$2^3P_{-1} \rightarrow 4^3D_{-2}$	$1^3(-1)^+ \rightarrow 2^3(-2)^+$	max
	20	4574	$2^3P_0 \rightarrow 4^3D_{-1}$	$1^30^- \rightarrow 2^3(-1)^-$	max

Table 1. continued

	B/MG	$\lambda/\text{Å}$	zero field trans.	transition	type
	17	4578	$4^3D_0 \rightarrow 2^3P_{+1}$	$5^30^+ \rightarrow 1^3(+1)^+$	max
	58	4711	$4^1D_0 \rightarrow 2^1P_{+1}$	$6^10^+ \rightarrow 1^1(+1)^+$	min
E:	251	4812	$2^1S_0 \rightarrow 3^1P_{-1}$	$2^10^+ \rightarrow 2^1(-1)^+$	min
	13	4993	$2^1P_{-1} \rightarrow 4^1D_{-2}$	$1^1(-1)^+ \rightarrow 2^1(-2)^+$	max
	18	5026	$4^1D_0 \rightarrow 2^1P_{+1}$	$6^10^+ \rightarrow 1^1(+1)^+$	max
	21	5056	$2^1P_0 \rightarrow 4^1D_{-1}$	$1^10^- \rightarrow 2^1(-1)^-$	max
A:	2109	5171	$2^1S_0 \rightarrow 3^1P_0$	$2^10^+ \rightarrow 2^10^-$	max
E:	47	5282	$2^1S_0 \rightarrow 3^1P_{-1}$	$2^10^+ \rightarrow 2^1(-1)^+$	max
D:	641	5600	$3^3S_0 \rightarrow 6^3P_0$	$2^30^+ \rightarrow 7^30^-$	min
D:	634	5810	$3^3S_0 \rightarrow 5^3F_0$	$2^30^+ \rightarrow 6^30^-$	min
D:	625	6199	$3^3S_0 \rightarrow 5^3P_0$	$2^30^+ \rightarrow 5^30^-$	min
B:	416	6267	$3^1S_0 \rightarrow 6^1F_0$	$3^10^+ \rightarrow 7^10^-$	min
	164	6314	$3^3D_0 \rightarrow 2^3P_{+1}$	$3^30^+ \rightarrow 1^3(+1)^+$	min
H:	681	6250	$3^3S_0 \rightarrow 5^3P_{-1}$	$2^30^+ \rightarrow 5^3(-1)^+$	min
	93	6513	$2^3P_{-1} \rightarrow 3^3D_{-2}$	$1^3(-1)^+ \rightarrow 1^3(-2)^+$	max
B:	416	6524	$3^1S_0 \rightarrow 5^1P_0$	$3^10^+ \rightarrow 6^10^-$	min
	91	6907	$3^3D_0 \rightarrow 2^3P_{+1}$	$3^30^+ \rightarrow 1^3(+1)^+$	max
B:	416	6978	$3^1S_0 \rightarrow 5^1F_0$	$3^10^+ \rightarrow 5^10^-$	min
D:	594	6998	$3^3S_0 \rightarrow 4^3F_0$	$2^30^+ \rightarrow 4^30^-$	min
	158	7051	$4^1S_0 \rightarrow 6^1P_{+1}$	$5^10^+ \rightarrow 9^1(+1)^+$	min
	258	7135	$2^3P_0 \rightarrow 3^3D_{-1}$	$1^30^- \rightarrow 1^3(-1)^-$	max
F:	499	7175	$3^1S_0 \rightarrow 5^1F_{-1}$	$3^10^+ \rightarrow 5^1(-1)^+$	min
H:	627	7426	$3^3S_0 \rightarrow 4^3F_{-1}$	$2^30^+ \rightarrow 4^3(-1)^+$	min
	68	7582	$4^1S_0 \rightarrow 6^1P_{+1}$	$5^10^+ \rightarrow 9^1(+1)^+$	max
	128	7632	$2^1P_{-1} \rightarrow 3^1D_{-2}$	$1^1(-1)^+ \rightarrow 1^1(-2)^+$	max
D:	4416	7641	$3^3S_0 \rightarrow 5^3P_0$	$2^30^+ \rightarrow 5^30^-$	max
B:	408	7923	$3^1S_0 \rightarrow 4^1P_0$	$3^10^+ \rightarrow 4^10^-$	min
H:	5029	8032	$3^3S_0 \rightarrow 5^3P_{-1}$	$2^30^+ \rightarrow 5^3(-1)^+$	max
H:	9	8467	$3^3S_0 \rightarrow 6^3P_{-1}$	$2^30^+ \rightarrow 7^3(-1)^+$	max
F:	458	8270	$3^1S_0 \rightarrow 4^1P_{-1}$	$3^10^+ \rightarrow 4^1(-1)^+$	min
B:	2253	8539	$3^1S_0 \rightarrow 5^1F_0$	$3^10^+ \rightarrow 5^10^-$	max
F:	2489	9003	$3^1S_0 \rightarrow 5^1F_{-1}$	$3^10^+ \rightarrow 5^1(-1)^+$	max
D:	5240	9180	$3^3S_0 \rightarrow 4^3F_0$	$2^30^+ \rightarrow 4^30^-$	max
D:	546	9348	$3^3S_0 \rightarrow 4^3P_0$	$2^30^+ \rightarrow 3^30^-$	min
	78	9434	$3^3D_0 \rightarrow 5^3F_0$	$3^30^+ \rightarrow 6^30^-$	min
H:	5	9521	$3^3S_0 \rightarrow 5^3F_{-1}$	$2^30^+ \rightarrow 6^3(-1)^+$	max
H:	31	9711	$3^3S_0 \rightarrow 5^3P_{-1}$	$2^30^+ \rightarrow 5^3(-1)^+$	max
	56	9730	$3^1D_0 \rightarrow 5^1P_0$	$4^10^+ \rightarrow 6^10^-$	min
F:	11	9829	$3^1S_0 \rightarrow 6^1F_{-1}$	$3^10^+ \rightarrow 7^1(-1)^+$	max
	88	9939	$3^3D_0 \rightarrow 5^3F_{-1}$	$3^30^+ \rightarrow 6^3(-1)^+$	min

Table 2. Crude estimates for the series limits calculated under the assumption that the differences in wavelengths divide by two for successive higher series members

	B/MG	$\lambda/\text{Å}$	transition	type
A:	490	2634	$2^10^+ \rightarrow \infty^10^-$	min
A:	1230	2710	$2^10^+ \rightarrow \infty^10^-$	max
B:	420	6010	$3^10^+ \rightarrow \infty^10^-$	min
C:	690	2093	$1^30^+ \rightarrow \infty^30^-$	min
C:	3080	2263	$1^30^+ \rightarrow \infty^30^-$	max
D:	650	5390	$2^30^+ \rightarrow \infty^30^-$	min
D:	3590	6102	$2^30^+ \rightarrow \infty^30^-$	max
E:	1450	2717	$2^10^+ \rightarrow \infty^1(-1)^+$	max
E:	610	2635	$2^10^+ \rightarrow \infty^1(-1)^+$	min
E:	4	3296	$2^10^+ \rightarrow \infty^1(-1)^+$	max
F:	540	6080	$3^10^+ \rightarrow \infty^1(-1)^+$	min
G:	3150	2253	$1^30^+ \rightarrow \infty^3(-1)^+$	max
G:	735	2100	$1^30^+ \rightarrow \infty^3(-1)^+$	min
G:	3	2722	$1^30^+ \rightarrow \infty^3(-1)^+$	max
H:	740	5074	$2^30^+ \rightarrow \infty^3(-1)^+$	min
H:	13	7413	$2^30^+ \rightarrow \infty^3(-1)^+$	max